

**Metal-Free Synthesis of Alternating Silylether–Carbosilane  
Copolymers Using Unsaturated Ketones**

Journal:	<i>Polymer Chemistry</i>
Manuscript ID	PY-ART-12-2023-001342.R1
Article Type:	Paper
Date Submitted by the Author:	02-Feb-2024
Complete List of Authors:	Yoshida, Naoki; Tohoku University Zhu, Huie; Tohoku University, Mitsuishi, Masaya; Tohoku University School of Engineering,

## ARTICLE

# Metal-Free Synthesis of Alternating Silylether–Carbosilane Copolymers Using Unsaturated Ketones

Naoki Yoshida, Huie Zhu,\* Masaya Mitsuishi\*

Received 00th January 20xx,  
Accepted 00th January 20xx

DOI: 10.1039/x0xx00000x

We report metal-free  $B(C_6F_5)_3$ -catalysed hydrosilylation polymerization for alternating silylether–carbosilane copolymers. The reaction was carried out at room temperature using bis(dimethylsilyl)benzene and cyclic and aliphatic unsaturated ketones. It was found that 1,4-conjugation on the unsaturated ketone monomers are important to undergo hydrosilylation-based polymerization on both C=O and C=C groups. The obtained polymers were characterized with high molecular weight ( $M_w = 4.23 \times 10^4$ , PDI = 2.0), tunable  $T_g$  (ranging from -7 to 27 °C) and good thermal stability (above 280 °C). Hydrolysis of the silylether linkages with HCl catalyst was demonstrated, revealing the alternating arrangement, which was supported by monitoring the polymerization processes with  $^1H$  NMR measurements.

## Introduction

Polymers containing Si–O or Si–C bonds in the main chain have recently attracted considerable interest in the development of new high-performance materials, including polysiloxanes, poly(silyl ether)s (PSEs) and polycarbosilanes (PCSs), etc. These hybrid polymeric materials usually show similar properties: low glass transition temperature, extreme flexibility, heat resistance and biocompatibility.<sup>1–5</sup> They can be applied as adhesives, paints and thermosets.<sup>6–11</sup> In particular, poly(silyl ether) (PSE) with Si–O–C bonds exhibits unique properties such as excellent thermal stability and optical transparency, which are not found in ordinary hydrocarbon polymers. In addition, silyl ether linkages of PSEs undergo hydrolysis with the aid of acid-catalyst, providing applications of degradable materials.<sup>12</sup> This characteristic differs from siloxanes, representative organosilicone materials; the main chains are completely decomposed upon acid-catalysed hydrolysis.<sup>13–17</sup>

Because of these valuable properties, several strategies have been developed for the synthesis of PSEs. The first attempt to synthesize PSEs involved the reaction of dichlorosilane with a diol in the presence of a base using an alcohol protection reaction.<sup>18</sup> However, the reaction tended to cause cyclization and yielded only oligomers having limited molecular weight. Reactions between monomers with dialkoxy groups and diaminosilanes were also carried out, but the reactions proceeded only in combination with diphenoxy groups and dianilinosilanes and were conducted at very high temperature (200~300 °C).<sup>19–23</sup> Since the 1990s, research on metal catalysts

became popular and various synthetic methods for PSE have been developed.<sup>24–30</sup> The first reaction in which high molecular weight PSE was synthesized was the condensation of disilane and diol using Pd/C as a catalyst.<sup>24</sup> In recent years, reactions without rare transition metals have been developed.<sup>13–15, 31–36</sup>

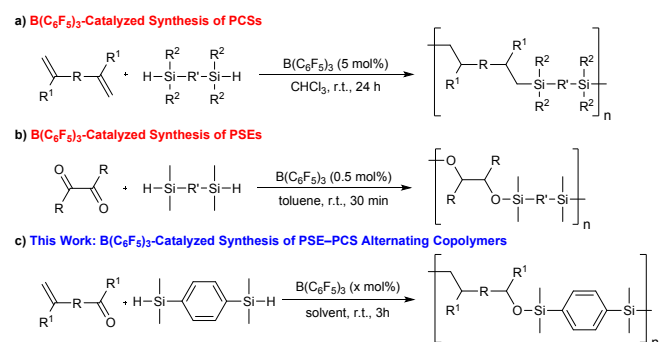
However, there are still challenging issues, e.g., high cost because of the use of rare transition metal complexes as reaction catalysts, degradation of physical properties of polymers due to residual metals such as coloration, formation of undesirable byproducts, and severe reaction conditions such as high temperature and long reaction time. Therefore, it is necessary to develop a novel method for synthesis of PSEs without transition metal catalysts under mild conditions.

Tris(pentafluorophenyl)borane ( $B(C_6F_5)_3$ ) can be used as a metal-free catalyst for hydrosilylation of alcohol,<sup>37</sup> ketone,<sup>38</sup> and olefin<sup>39</sup> in high yields with low catalyst loading. It can also be used for other hydrosilylation reactions such as aromatic C–H bond hydrosilylation<sup>40</sup> and silicon-sulfur bond formation reactions.<sup>41</sup> Chang and co-workers first reported a  $B(C_6F_5)_3$ -catalyzed synthesis of PCSs with diene and disilane at room temperature (Scheme 1a).<sup>42</sup> In addition, Hawker and co-workers demonstrated that  $B(C_6F_5)_3$  catalyst enabled rapid polymerization of  $\alpha$ -diketone and disilane monomers under ambient conditions, yielding high molecular weight PSEs (Scheme 1b).<sup>43</sup> However, there are few reports about hydrosilylation polymerization of hybrid polymers using  $B(C_6F_5)_3$ .<sup>44–46</sup>

In this study, we explored direct synthesis of new hybrid polymers with alternating Si–O–C and Si–C bonds in the polymer backbones using commercially available unsaturated ketones as monomers, which have both vinyl and carbonyl reactive groups in the chemical structure for  $B(C_6F_5)_3$ -catalyzed hydrosilylation reaction (Scheme 1c). Reaction mechanisms, polymer properties, and their degradation properties were also investigated.

Graduate School of Engineering, Tohoku University, 6-6-11 Aramaki Aza Aoba, Aoba-ku, Sendai 980-8579, Japan.

† Footnotes relating to the title and/or authors should appear here.  
Electronic Supplementary Information (ESI) available: [details of any supplementary information available should be included here]. See DOI: 10.1039/x0xx00000x

Scheme 1. Synthetic methods of PSE and PCS with  $B(C_6F_5)_3$  catalyst

## Experimental

### Materials

2-Cyclopenten-1-one (CP) and 2-cyclohexen-1-one (CH), 2-cyclohepten-1-one, dimethylphenylsilane (DMPS), 1,4-bis(dimethylsilyl)benzene (DMSB), *trans*-benzalacetone (TBA) (*E*)-4-hexen-3-one (4H3o), dibromomethane and tris(pentafluorophenyl)borane ( $B(C_6F_5)_3$ ) were purchased from Tokyo Chemical Industry Co., Ltd. Anhydrous toluene and anhydrous chloroform, anhydrous dichloromethane, anhydrous cyclohexane, anhydrous acetonitrile and active alumina were purchased from Fujifilm Wako Pure Chemical Industries Ltd. Deuterated chloroform was purchased from Kanto Chemical Co., Inc. All chemical materials were used without further purification.

### Methods

Nuclear Magnetic Resonance (NMR) measurements were performed using a 400 MHz NMR spectrometer (AVANCE III; Bruker Analytik). All samples were dissolved in  $CDCl_3$  and chemical shifts ( $\delta$ ) are reported in ppm relative to the residual proton signal of the dehydrated solvent as appropriate. Infrared (IR) spectra were recorded on a Fourier-transform infrared (FT-IR) spectrometer (FT/IR4200; Jasco Corp.).  $CaF_2$  ( $1 \times 2.5 \text{ cm}^2$ ) substrates were used for FT-IR measurements after washing in chloroform, acetone and 2-propanol in order. Then they were dried by  $N_2$  flow. Size exclusion chromatography (SEC) measurements were taken using a GPC system (GPC-8020; Tosoh Corp.) equipped with a gel column (TSK gel SuperH2M-M; Tosoh Corp.) and refractive index (RI) and UV detectors (RI-8020 and UV-8020) using polystyrene standards. Differential scanning calorimetry (DSC) measurement was performed using a DSC system (DSC-60; Shimadzu Corp.) at a scanning rate of  $10 \text{ }^\circ\text{C min}^{-1}$  from  $-140 \text{ }^\circ\text{C}$  to  $200 \text{ }^\circ\text{C}$  under a nitrogen atmosphere. Thermogravimetric analysis (TGA) was performed (Thermo plus2; Rigaku) with a heating rate of  $10 \text{ }^\circ\text{C min}^{-1}$  from  $20 \text{ }^\circ\text{C}$  to  $1000 \text{ }^\circ\text{C}$  under an argon atmosphere.

### Model reaction

In a glass vial equipped with a Teflon coated stir bar, CP and DMPS were added to a solution of  $B(C_6F_5)_3$  in dehydrated toluene under nitrogen atmosphere, and the reaction mixture was stirred at room temperature for 1 h. Then, activated

alumina was added to the resulting solution to remove  $B(C_6F_5)_3$  and stop the reaction. After filtering off the activated alumina, the solvent was removed with rotary evaporator and dried in a vacuum oven. The obtained solution was investigated by NMR spectroscopy. The yield of the product was determined by  $^1\text{H}$  NMR analysis using  $CH_2Br_2$  as the internal standards.  $^1\text{H}$  NMR (400 MHz,  $CDCl_3$ ):  $\delta$  7.79–7.78 (dd, 2H), 7.74–7.72 (dd, 2H), 7.59–7.55 (m, 6H), 4.73 (ddd, 1H), 2.04–1.91 (m, 3H), 1.83–1.79 (m, 2H), 1.74–1.70 (m, 1H), 1.54 (ddd, 1H), 0.60 (s, 3H), 0.55 (s, 6H), 0.54 (s, 3H).  $^{13}\text{C}$  NMR (400 MHz,  $CDCl_3$ ):  $\delta$  140.77, 138.73, 133.93, 133.61, 129.41, 128.53, 127.75, 127.64, 77.78, 37.48, 34.89, 26.35, 24.69, -0.62, -1.46, -2.35, -2.91.  $^{29}\text{Si}$  NMR (400 MHz,  $CDCl_3$ ):  $\delta$  3.94, -3.69.

### Representative polymer synthesis

In a glass vial equipped with a Teflon coated stir bar, CP and DMSB were added to a solution of  $B(C_6F_5)_3$  in dehydrated solvent under nitrogen atmosphere, and the reaction mixture was stirred at room temperature. Then, activated alumina was added to the resulting solution to remove  $B(C_6F_5)_3$  and stop the reaction. After filtering off the activated alumina, the solvent was removed with rotary evaporator and the product was purified through reprecipitation. As all of the polymers were soluble in dichloromethane and insoluble in methanol, these two solvents were used in the reprecipitation process. The final precipitate was isolated and dried in a vacuum oven to give the polymers.  $^1\text{H}$  NMR (400 MHz,  $CDCl_3$ ):  $\delta$  7.77–7.68 (m, 4H), 4.70 (d, 1H), 1.97–1.89 (m, 3H), 1.77 (m, 2H), 1.68 (m, 1H), 1.50 (m, 1H), 0.61–0.49 (m, 12H).  $^{13}\text{C}$  NMR (400 MHz,  $CDCl_3$ ):  $\delta$  133.19, 132.81, 129.21, 128.41, 77.88, 37.59, 34.91, 26.47, 24.80, -0.58, -1.51, -2.32, -2.80.  $^{29}\text{Si}$  NMR (400 MHz,  $CDCl_3$ ):  $\delta$  5.13, -2.60.

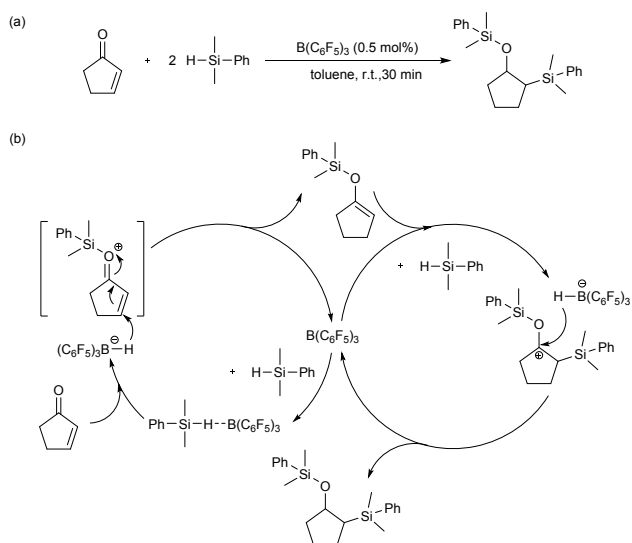
### Hydrolytic degradation of CP–DMSB

CP–DMSB (10 mg) and THF (1 mL) were added to a glass vial equipped with a Teflon coated stir bar. After getting homogeneous solution, calculated volumes of distilled  $H_2O$  or HCl aq. (pH = 2.0) were added to the reaction mixture at room temperature. Samples were taken at specific times and diluted for molecular weight determination.

## Results and discussion

Piers et al. developed borane-catalyzed 1,4-hydrosilylation of  $\alpha$ ,  $\beta$ -unsaturated ketones<sup>47</sup> and promoted a series of small molecule studies to define the reaction scope and optimized conditions. In order to confirm the desired polymerization reaction progress, a model reaction of 2-cyclopenten-1-one (CP) and dimethylphenylsilane (DMPS) was investigated under ambient conditions (Scheme 2a). The hydrosilylation of CP was achieved within 30 min using minuscule amount (0.5 mol%) of the  $B(C_6F_5)_3$  catalyst, resulting in yields up to 80% in a single step. The mechanism of this reaction is proposed as shown in Scheme 2(b). First, the reaction is initiated by the borane catalyst which activates the Si-H bond to generate the hydride and corresponding silyl cation. The reaction with the carbonyl group first yields the silyl enol ether, and then the silyl cation reacts with the C=C bond to give the desired product.

Scheme 2. (a) Model reaction of CP and DMPS. (b) Plausible reaction mechanism for hydrosilylation of CP with DMPS.



On the basis of this metal-free hydrosilylation, we subsequently studied the reaction between CP and 1,4-bis(dimethylsilyl)benzene (DMSB) as a model step-growth polymerization system (Table 1). Low catalyst loading (0.5 mol%) equimolar conditions in toluene yielded alternating silylether-carbosilane copolymer with a weight-average molecular weight of  $M_w = 1.31 \times 10^4$  (entry 1, 40% yield). The polydispersity index (PDI) value is approximately 2.0, which is consistent with the PDI value characteristic of step-growth polymerization. Reducing the CP equivalent to 0.90 or 0.95 results in higher molecular weights, but the PDI values became larger (entries 2 and 3). This is because of the presence of the excessive Si-H bonds in the reaction system, leading to side reactions such as the formation of silphenylene silicones, attributed to the nucleophilic attack on silyl-ether oxygen by excessive silyl cations (e.g., product E, Scheme S1). In contrast, when the CP equivalent increased, the molecular weight became relatively lower; polymers were capped by excess CP monomers at each chain end, which was unfavourable for hydrosilylation polymerization (Fig. S2). The PDI value became lower as the molecular weight decreased.

Decrease in the catalyst loading to 0.25 mol% results in approximately 2.5 times higher molecular weight ( $M_w = 3.34 \times 10^4$ , entry 6) than those obtained at 0.5 mol% catalyst loading, indicating that  $\text{B(C}_6\text{F}_5)_3$  regenerates effectively during polymerization. However, the molecular weight decreased to  $M_w = 8.92 \times 10^3$ , when the catalyst loading was 5 mol%. The result can be attributed to side reactions and decomposition reactions. No polymerization was observed when the polymerization was carried out with total monomer concentration of 0.25 M (1/8 of the monomer concentration in Table 1) for all the comonomers at 0.25 mol% loading.

To examine the conformation of the CP-DMSB main chain next to the cyclopentane ring, the spin-spin coupling constants of the products of the model reaction were analysed using  $^1\text{H}$  NMR spectra, and the vicinal spin-spin coupling constant for

Table 1. Effect of the feeding ratio and catalyst loading on  $\text{B(C}_6\text{F}_5)_3$  hydrosilylation polymerization<sup>a</sup>

entry	CP [equiv.]	x [mol%]	$M_n^b / 10^3$	$M_w^b / 10^3$	$M_w / M_n^b$	Yield [%] <sup>c</sup>
1	1.0	0.5	5.90	13.1	2.2	39
2	0.90	0.5	8.64	33.9	3.9	48
3	0.95	0.5	17.8	66.2	3.7	52
4	1.05	0.5	4.82	12.6	2.6	42
5	1.10	0.5	5.30	10.5	2.0	28
6	1.0	0.25	18.5	33.4	1.8	57
7	1.0	1	9.98	16.6	1.7	39
8	1.0	5	6.97	8.92	1.3	4

<sup>a</sup>Polymerization conditions: CP (1.0 mmol), DMSB (1.0 mmol) and  $\text{B(C}_6\text{F}_5)_3$  (0.5 mol%) in 1.0 mL of toluene. <sup>b</sup>Determined using SEC calibrated with polystyrene standards in THF with a flow rate of 0.2 mL  $\text{min}^{-1}$  at 40 °C. <sup>c</sup>Isolated yield.

the following structure was determined as  $^3J_{\text{HH}} = 5.5$  Hz (Fig. 1(a)). From this value and the Karplus equation (eq. 1),<sup>47-49</sup> the dihedral angle between  $\text{H}_a$  and  $\text{H}_b$  was determined as  $44^\circ$  (Fig. 1(b)). As Piers et al. pointed out,<sup>47</sup> selective attack of the hydride *trans* to the bulky silyl group leads to the *cis* products in  $\text{B(C}_6\text{F}_5)_3$ -catalyzed hydrosilylation of silyl enol ethers. The result infers that the polymer main chain takes a gauche-kink conformation shown in Fig.1(c) and (d).

$$^3J_{\text{HH}} = A \sin^2 \theta + B \cos \theta + C \quad (A = 9.4, B = -1.4, C = 1.6) \quad (1)$$

Effects of reaction solvent on the polymerization were examined using 0.25 mol%  $\text{B(C}_6\text{F}_5)_3$  as catalyst (Table 2). When nonpolar cyclohexane was used as a solvent, the molecular

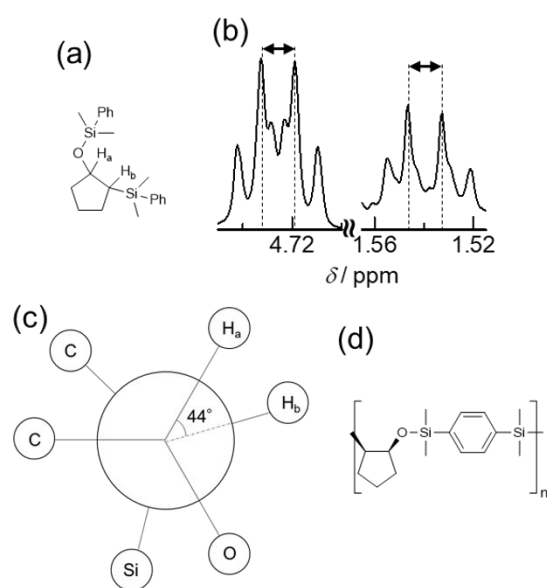
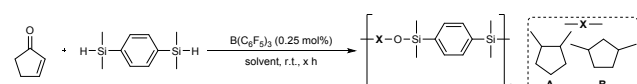


Fig. 1 (a) Chemical structure of the product obtained through model reaction. (b)  $^1\text{H}$  NMR spectra of  $\text{H}_a$ (left) and  $\text{H}_b$ (right). (c) Newman projection of the product around the C-C axis of cyclopentane. (d) Predicted structure of CP-DMSB.

weight ( $M_w = 3.03 \times 10^4$ ) of the obtained polymer was comparable to that of the polymer using toluene ( $M_w = 3.34 \times 10^4$ ) (entries 1 and 2 in Table 2). As the solvent polarity increased, the molecular weight decreased; when acetonitrile was used, the polymerization reaction did not proceed (entries 3–5).

According to the reaction mechanism (Scheme 2), two types of main chain structures (A and B) are possible through 1,2-addition and 1,4-addition, respectively, which are confirmed using  $^1\text{H}$  COSY NMR (Fig. S11). These two types of chain structures were attributed to cation shift (Scheme 3). Other than chloroform (entry 4 in Table 2), polymers synthesized in nonpolar solvents were found to have the A structure more than 90%. In nonpolar solvents such as cyclohexane and toluene, the reaction proceeds immediately to the second hydrosilylation step because the silyl enol ether products are themselves susceptible to hydrosilylation. Therefore, the main chain backbone of the 1,2-adduct with a structure of silyl enol ether, was preferably formed. In contrast, the cationic intermediates are relatively stabilized in chloroform, thus cationic transitions are more likely to occur, leading to the increase in the 1,4-adduct ratio. The lower molecular weight in chloroform is due to the lower proportion of silyl enol ethers, which are more reactive than alkenes as reaction intermediates, making it more difficult for the second step reaction to proceed. It is noteworthy that the ratio of 1,2- and 1,4-adducts for the model reaction (Scheme 2(a)) was the same as that of the corresponding polymerization. However, the 1,2- and 1,4-product ratio was 56 : 44 for the model reaction in chloroform, while it was 86 : 14 for the polymerization in chloroform. This means that 1,2-adducts are preferable for hydrosilylation-based polymerization.

Table 2. Effect of reaction solvents and reaction time on  $\text{B}(\text{C}_6\text{F}_5)_3$  catalyzed hydrosilylation polymerization<sup>a</sup>

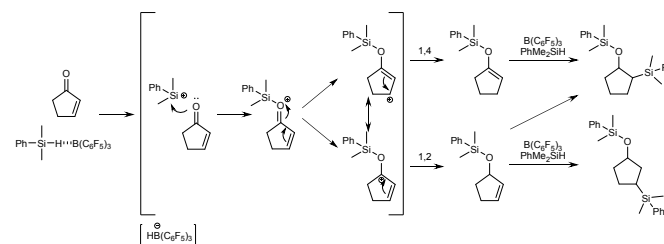


entry	solvent	time [h]	$M_n^b / 10^3$	$M_w^b / 10^3$	$M_w / M_n^b$	A : B <sup>c</sup>	yield [%] <sup>d</sup>
1	cyclohexane	1	17.0	30.3	1.8	90 : 10	58
2	toluene	1	18.5	33.4	1.8	94 : 6	57
3	$\text{CH}_2\text{Cl}_2$	1	6.10	13.5	2.2	94 : 6	46
4	$\text{CHCl}_3$	1	1.69	3.20	1.9	86 : 14	21
5 <sup>e</sup>	$\text{CH}_3\text{CN}$	1	-	-	-	-	-
6	toluene	0.5	11.0	16.8	1.5	92 : 8	45
7	toluene	3	21.3	42.3	2.0	96 : 4	51
8	toluene	5	17.0	34.9	2.1	92 : 8	63
9	toluene	24	14.5	25.3	1.7	91 : 9	61

<sup>a</sup>Polymerization conditions: CP (2.0 mmol), DMSB (2.0 mmol) and  $\text{B}(\text{C}_6\text{F}_5)_3$  in 2.0 mL of solvent. <sup>b</sup>Determined by SEC calibrated by polystyrene standards in THF with a flow rate of 0.2 mL  $\text{min}^{-1}$  at 40 °C. <sup>c</sup>Ratio of A : B determined using  $^1\text{H}$  NMR. <sup>d</sup>Isolated yield. <sup>e</sup>Not polymerized.

For entries 2, 6–9 (Table 2), effects of the reaction time on polymerization were also observed. It was found that longer reaction times are required to increase the molecular weight.

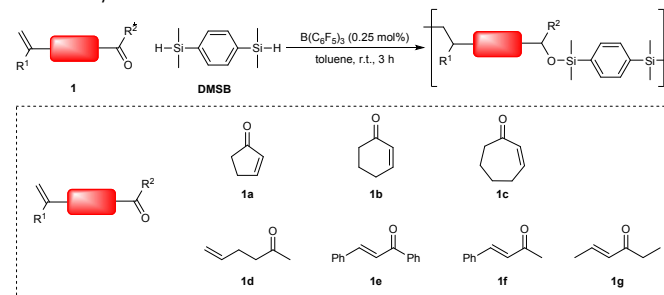
Scheme 3. Plausible reaction mechanism for two types of products by 1,2- or 1,4-addition.



When the reaction time increased from 0.5 to 3 h, the desired polymer with the highest molecular weight was obtained (entry 7). However, further extension of the reaction time resulted in a slight decrease in the molecular weight (entries 8–9). This is probably due to the decomposition of the silyl ether bond as a side reaction (Scheme S1, Table S1, and Fig. S13).

Different  $\alpha,\beta$ -unsaturated ketones commercially available were reacted with DMSB to explore the reaction activities (Table 3). The desired reaction was also confirmed using DMSB and 2-cyclohexen-1-one (1b), which has a larger ring size than that of CP. The final product has a molecular weight of approximately  $6.00 \times 10^3$ , indicating oligomer formation. When 2-cyclohepten-1-one (1c) was used as a monomer, the polymerization did not proceed and only silyl enol ether was obtained as the reaction intermediate. This implies that the planarity of the cycloalkane affects the second hydrosilylation step; the 2-cyclohepten-1-one ring takes a nonplanar conformation because of more torsional strain, compared with

Table 3. Polymerization of various unsaturated ketones and DMSB.<sup>a</sup>



entry	unsaturated ketone	$M_n^b / 10^3$	$M_w^b / 10^3$	$M_w / M_n^b$	yield [%] <sup>c</sup>	$T_g$ [°C] <sup>d</sup>	$T_{d5}$ [°C] <sup>d</sup>
1	<b>1a</b>	21.3	42.3	2.0	40	13	322
2	<b>1b</b>	5.25	6.03	1.9	64	8	316
3	<b>1c</b>	-	-	-	-	-	-
4	<b>1d</b>	-	-	-	-	-	-
5	<b>1e</b>	-	-	-	-	-	-
6	<b>1f</b>	4.82	6.42	1.3	24	-7	314
7 <sup>f</sup>	<b>1g</b>	2.03	2.42	1.2	9	27 <sup>g</sup>	289

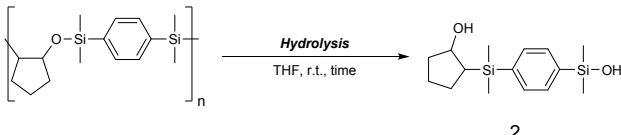
<sup>a</sup>Polymerization conditions: unsaturated ketone (2.0 mmol), DMSB (2.0 mmol) and  $\text{B}(\text{C}_6\text{F}_5)_3$  (0.025 mmol) in 2.0 mL of toluene. <sup>b</sup>Determined using SEC calibrated by polystyrene standards in THF with a flow rate of 0.2 mL  $\text{min}^{-1}$  at 40 °C. <sup>c</sup>Isolated yield. <sup>d</sup>Glass transition temperatures ( $T_g$ ) were measured via differential scanning calorimetry (DSC). <sup>e</sup>Thermal decomposition temperature ( $T_{d5}$ ) was measured using thermogravimetric analysis (TGA) and  $T_{d5}$  denotes the temperature at 5% mass loss under nitrogen. <sup>f</sup> $\text{B}(\text{C}_6\text{F}_5)_3$  (0.025 mmol) was used as catalyst and the reaction time was 5h. <sup>g</sup>melting point: 94 °C.

the cyclopentene and cyclohexene rings. Next, with 5-hexen-2-one (1d) as the noncyclic unsaturated ketone, only the carbonyl group reacted to give the silyl ether, while the vinyl group remained unreacted even when the reaction time was further extended, and the reaction between the silyl cation and the silyl ether oxygen produced the silphenylene silicone. Therefore, it is necessary to go through a highly active silyl enol ether intermediate for the desired polymerization to proceed. Then, when noncyclic unsaturated ketone chalcone (1e) was used, polymerization did not proceed and the reaction intermediate silyl enol ether and the reduced form, ketone, were obtained (Scheme S1 and Table S1).<sup>50</sup> When DMSB was reacted with *trans*-benzalacetone (1f), however, polymerization proceeded to generate alternating silyl ether-carbosilane copolymers. In this case, the steric hindrance of the adjacent substituent to the unsaturated bond is small for the reaction to proceed. (*E*)-4-hexen-3-one (4H3o) (1g) was reacted with DMSB for 3h, for which a silyl enol ether with unreacted alkene moieties was produced and a part of Si–H bonds remained unreacted. When the catalyst amount and the reaction time were increased, the desired product was also obtained (entry 7). Results indicate that smaller steric hindrance of the substituent adjacent to the carbonyl group is beneficial for the polymerization to proceed.

In addition, we investigated the thermal properties of the alternating silylether–carbosilane copolymers using differential scanning calorimetry (DSC) and thermal gravimetric analysis (TGA) (Fig. S14 and S15). Because of the flexibility of silyl ether bonds, the glass transition temperature ( $T_g$ ) of the final polymers ranged from -7 to 27 °C and the melting temperature was observed only for 4H3o–DMSB. All polymers were demonstrated with a thermal decomposition temperature ( $T_{ds}$ ) above 280 °C, showing excellent thermal stability. As shown in the TGA curves of the copolymers (Fig. S15), there are two weight loss processes in the TGA curves. The first sharp decrease at 300 ~ 400 °C is caused by the decomposition of the cyclopentane ring in the main chain, and the second sharp decrease at 500 ~ 600 °C is assigned to the decomposition of the aromatic ring in the main chain. The char yield was determined as 20 wt% at 1000 °C, which may originate from ceramic formation of the hybrid polymers under heating.

Hydrolytic properties of the silylether (Si–O–C) bonds in PSEs are useful for the applications as recyclable/sustainable materials. For investigating the degradability of the alternating silylether–carbosilane copolymer, CP–DMSB was chosen because of the highest molecular weight. After dissolving CP–DMSB in THF, H<sub>2</sub>O or HCl/H<sub>2</sub>O was added to the solution and the solution was stirred under room temperature. Then, we monitored changes in the molecular weight of CP–DMSB using SEC as functions of the acid catalyst loading and hydrolysis time (Table 4). Firstly, by only adding 2 vol% H<sub>2</sub>O, no change in the molecular weight was observed even after 24 h. This is in good consistent with that of other earlier reports for PSEs,<sup>13–17</sup> suggesting that the silyl ether linkage is stable against a small amount of H<sub>2</sub>O. When HCl aqueous solution (pH = 2.0) was added (2 vol% relative to the polymer solution) and the solution was stirred for 24 h, the molecular weight decreased (Fig. S16). The decrease in the molecular weight is

Table 4. Hydrolysis of CP–DMSB under various degradation conditions.<sup>a</sup>



Degradation condition	quant. [vol%]	time [h]	$M_n^b / 10^3$	$M_w^b / 10^3$	$M_w / M_n^b$
Original	-	-	21.3	40.2	2.0
H <sub>2</sub> O	2	24	19.5	39.0	2.0
	2	24	17.3	33.6	1.9
HCl aq. (pH = 2.0)	2	72	14.6	28.1	1.9
	10	72	<2.00	<2.00	-

<sup>a</sup>Degradation conditions: CP–DMSB (10 mg) and H<sub>2</sub>O or HCl aq. in 1.0 mL of THF.

<sup>b</sup>Determined using SEC calibrated by polystyrene standards in THF with a flow rate of 0.2 mL min<sup>-1</sup> at 40 °C.

less than that of PSEs at the same condition in earlier reports,<sup>13–17</sup> indicating that the alternating silylether–carbosilane of the CP–DMSB has more hydrophobic nature and it becomes less degradable. When the reaction time was extended to 72 h, the molecular weight decreased further, but CP–DMSB still remained undecomposed with a molecular weight of  $2.80 \times 10^4$ . The SEC curve (red, Fig. S16) shows that degradation progressed, and the molecular weight peak shifted to the lower molecular weight region and a new peak appeared as the low-molecular weight components generated by hydrolysis. As the SEC curve (blue, Fig. S16) for the 72 h hydrolyzed polymer by adding 10 vol% HCl (aq.) shows, the high molecular weight peak almost disappeared with appearance of several new peaks in the low molecular weight region. This indicates that the degradation of CP–DMSB completed by adding 10 vol% HCl aqueous solution for 72 h.

Interestingly, more than 95 % of the decomposed components consist of repeating unit-based diol (2 in Table 4 (90 % yield)), which was confirmed using <sup>1</sup>H NMR and FT-IR, indicating that CP–DMSB has alternating patterns in itself. Fig. S17 shows the <sup>1</sup>H NMR spectra measured after 10 vol% of HCl solution (pH 2) was added as acid catalyst and stirred for 72 h. FT-IR measurements (Fig. S18) clarifies that the hydrolysis product had silanol and alcohol groups. Since the hydrolysis product are produced only when the silyl ether and carbosilane bonds in the copolymer are connected alternately, the result suggests strongly that the synthesized polymer is an alternating copolymer. It is noteworthy that repolymerization is possible using diol 2 in the B(C<sub>6</sub>F<sub>5</sub>)<sub>3</sub> catalyzed reaction system (Fig. S19).

As reported in earlier reports, poly(silyl ether)s form more easily than polycarbosilanes:<sup>42,43</sup> (polymerization time) 30 min vs. 24 h; (B(C<sub>6</sub>F<sub>5</sub>)<sub>3</sub> loading) 0.5 mol% vs. 5 mol%, for Si–O and Si–C bond formation, respectively. The alternating arrangement of CP–DMSB was examined by tracking the B(C<sub>6</sub>F<sub>5</sub>)<sub>3</sub>-catalysed hydrosilylation polymerization using <sup>1</sup>H NMR. We monitored the polymerization with a total monomer concentration of 0.5 M (Fig. S20). The reaction did not proceed until 10 min, and CP–DMSB dimers with silyl enol ether–silane linkage alone were observed as the reaction intermediate at 15 min. Then new signals responsible for polymer components appeared at 60

min. Most of the reaction intermediates were consumed and the polymerization was completed in 90 min. In order to understand the reaction intermediates, we investigated the intermediate structures by varying the feed ratio of CP and DMSB from 1:1 to 2:1 for 1 h (Fig. S21). In the case of 1.0 or 1.1 equivalents of CP to DMSB, copolymer components with alternating patterns were observed. As the feed ratio increased, another peak appeared in the NMR spectra, which suggested double-ended silyl enol ether formation. When the CP ratio was increased to 2.0 equivalents, double ended silyl enol ethers became significant; miniscule amounts of polymers generated. Results indicate that hydrosilylation did not proceed concomitantly at the both ends of DMSB because of bulkiness of  $B(C_6F_5)_3$  and that a bis-silyl cation does not form because of low catalyst concentration. As a consequence, the reaction intermediate consisting of CP and DMSB serves as a repeating unit. In the case of 1:1 feed ratio, step-growth polymerization proceeds so that the copolymer backbone has alternating arrangement. The reaction yield of the CP-DMSB unit is not so high (80%), but this might affect the suppression of the "CP-DMSB-CP" component formation through the reaction of two equivalents of CPs with DMSB. In the case of 2:1 feed ratio, however, excess  $\alpha,\beta$ -unsaturated ketone CP underwent hydrosilylation with DPSB, resulting in double ended silyl enol ether formation. Therefore, in this polymerization reaction, rather than the alternating step-by-step reaction between  $\alpha,\beta$ -unsaturated ketones and disilanes to elongate the molecules, silyl enol ether-silane intermediates formation, in which only the highly reactive carbonyl group underwent hydrosilylation reaction, *i.e.*, only one of the Si-H bonds of DPSB reacted first, became preferential, and then the polymerization reaction of the intermediates proceeded.

## Conclusions

We investigated hydrosilylation polymerization of  $\alpha, \beta$ -unsaturated ketones with disilanes using metal-free Lewis acid catalyst  $B(C_6F_5)_3$ . Under low catalyst loading and mild condition, alternating silylether-carbosilane copolymers were successfully synthesized using commercially available unsaturated ketones and disilanes as monomers through a one-pot reaction:  $M_w = 4.23 \times 10^4$  ( $M_w/M_n = 2.0$ ) through optimization of the hydrosilylation reaction conditions including the monomer ratio (CP : DMSB = 1 : 1), catalyst loading (0.25 %), solvent type (toluene), and reaction time (3 h) in the metal-free  $B(C_6F_5)_3$  catalyzed reaction system. Our strategies demonstrated that conjugated enones are important for  $B(C_6F_5)_3$  catalyzed polymerization with 1,4-hydrosilylation followed by hydrosilylation of silyl enol ethers. The obtained copolymers were found to have low glass transition temperature ranging -7 to 27 °C and high thermal stability characteristics similar to common PSEs. Of all the obtained polymers, CP-DMSB copolymers were investigated for confirmation of their hydrolysis properties. It was found that complete hydrolysis was possible by adding 10 vol% HCl aq.; polymer chains were decomposed into corresponding silanol and hydroxyl products

through cleavage of silyl ether linkages. The results support the alternating arrangement of CP-DMSB copolymers. The alternating patterns were also confirmed by tracking the reaction using  $^1H$  NMR. It is noteworthy that hydrolysis products were recyclable for repolymerization.

In this study, alternating silylether-carbosilane copolymers exhibited relatively low molecular weights. Considering the molecular weight and the yield of polycarbosilanes are  $M_n = 1.41 \times 10^4$  and < 54 % respectively,<sup>43</sup> the result is reasonable. Interestingly, the molecular weight ranges  $M_w \sim 10^4$ , though the reaction yield of the comonomers in the model reaction is moderate (80 %). We chose DMSB as reactive disilane comonomers. It is noteworthy that no polymerization was observed using 1,1,3,3-tetramethyldisiloxane in toluene; the reactivity of disilanes are important for  $B(C_6F_5)_3$ -catalyzed hydrosilylation polymerization for alternating copolymer formation. For example, cyclosiloxanes and aromatic disilanes are available for polymerization (Table S2 and Fig. S22). Work related to the polymerization details for these comonomers are now in progress.

## Conflicts of interest

There are no conflicts to declare.

## Acknowledgements

The work was partially supported by Grants-in-Aid for Early Career Scientists (19K15625) from the Japan Society for the Promotion of Science (JSPS). The work was also supported by the Cooperative Research Program "Network Joint Research Center for Materials and Devices": Dynamic Alliance for Open Innovation Bridging Human, Environment and Materials (MEXT). N.Y. is grateful to the financial support from Advanced Graduate School Training/Career-Building Programs (JPMJSP2114), Japan Science and Technology Agency. H. Z. appreciates support from Tohoku University Center for Gender Equality Promotion (TUMUG), PHYM Center Project, Tohoku University.

## Notes and references

- J. E. Curry and J. D. Byrd, *J. Appl. Polym. Sci.*, 1965, 9, 295–311.
- D. Fallahi, H. Mirzadeh and M. T. Khorasani, *J. Appl. Polym. Sci.*, 2003, 88, 2522–2529.
- M. Zielecka and E. Bujnowska, *Prog. Org. Coat.*, 2006, 55, 160–167.
- E. Yilgör and I. Yilgör, *Prog. Polym. Sci.*, 2014, 39, 1165–1195.
- S. Luleburgaz, U. Tunca, and H. Durmaz, *Polym. Chem.*, 2023, 14, 2949–2957.
- A. Demirci, S. Yamamoto, J. Matsui, T. Miyashita and M. Mitsuishi, *Polym. Chem.*, 2015, 6, 2695–2706.
- P. R. Dvornic and R. W. Lenz, *Macromolecules*, 1994, 27, 5833–5838.
- M. Birot, J.-P. Pillot and J. Dunogues, *Chem. Rev.*, 1995, 95, 1443–1477.
- S. Putzien, O. Nuyken and F. E. Kühn, *Prog. Polym. Sci.*, 2010, 35, 687–713.
- J. M. Buriak, *Chem. Mater.*, 2014, 26, 763–772.

- 11 S. Gao, Y. Liu, S. Feng and Z. Lu, *J. Mater. Chem. A*, 2019, 7, 17498–17504.
- 12 X. Yan, L. Bai, B. Feng and J. Zheng, *Eur. Polym. J.*, 2022, 173, 111267–111278.
- 13 C. M. Bunton, Z. M. Bassampour, J. M. Boothby, A. N. Smith, J. V. Rose, D. M. Nguyen, T. H. Ware, K. G. Csaky, A. R. Lippert, N. V. Tsarevsky and D. Y. Son, *Macromolecules*, 2020, 53, 9890–9900.
- 14 C. Cheng, A. Watts, M. A. Hillmyer and J. F. Hartwig, *Angew. Chem. Int. Ed.*, 2016, 55, 11872–11876.
- 15 S. Vijjamarri, S. Streed, E. M. Serum, M. P. Sibi and G. Du, *ACS Sustainable Chem. Eng.*, 2018, 6, 2491–2497.
- 16 S. Vijjamarri, M. Hull, E. Kolodka and G. Du, *ChemSusChem*, 2018, 11, 2881–2888.
- 17 C. S. Sample, S.-H. Lee, M. W. Bates, J. M. Ren, J. Lawrence, V. Lensch, J. A. Gerbec, C. M. Bates, S. Li and C. J. Hawker, *Macromolecules*, 2019, 52, 1993–1999.
- 18 H. Fouilloux, M.-N. Rager, P. Ríos, S. Conejero and C. M. Thomas, *Angew. Chem. Int. Ed.*, 2021, e202113443.
- 19 R. H. Kriebel and C. A. Burkhard, *J. Am. Chem. Soc.*, 1947, 69, 2689–2692.
- 20 F. A. Hengle and P. Schulder, *Makromol. Chem.*, 1954, 13, 53–70.
- 21 W. R. Dunnavant, R. A. Markle, P. B. Stickney, J. E. Curry and J. D. Byrd, *J. Polym. Sci. Part A: Polym. Chem.*, 1967, 5, 707–724.
- 22 W. R. Dunnavant, R. A. Markle, R. G. Sinclair, P. B. Stickney, J. E. Curry, J. D. Byrd, *Macromolecules*, 1968, 1, 249–254.
- 23 M. Padmanaban, M.-A. Kakimoto and Y. Imai, *J. Polym. Sci. Part A: Polym. Chem.*, 1989, 28, 2997–3005.
- 24 Y. Imai, *J. Macromol. Sci. Chem.*, 1991, 28, 1115–1135.
- 25 Y. Li and Y. Kawakami, *Macromolecules*, 1999, 32, 8768–8773.
- 26 J. K. Paulasaari and W. P. Weber, *Macromolecules*, 1998, 31, 7105–7107.
- 27 Y. Li and Y. Kawakami, *Macromolecules*, 1999, 32, 6871–6873.
- 28 J. M. Mabry, J. K. Paulasaari and W. P. Weber, *Polymer*, 2000, 41, 4423–4428.
- 29 J. M. Mabry, M. K. Runyon and W. P. Weber, *Macromolecules*, 2001, 34, 7264–7268.
- 30 G. Lázaro, M. Iglesias, F. J. Fernández-Alvarez, P. S. Miguel, J. J. Pérez-Torrente and L. A. Oro, *ChemCatChem*, 2013, 5, 1133–1141.
- 31 G. Lázaro, F. J. Fernández-Alvarez, M. Iglesias, C. Horna, E. Vispe, R. Sancho, F. J. Lahoz, M. Iglesias, J. J. Pérez-Torrente and L. A. Oro, *Catal. Sci. Technol.*, 2014, 4, 62–70.
- 32 C. Lichtenberg, M. Adelhardt, M. Wörle, T. Büttner, K. Meyer and H. Grützmacher, *Organometallics*, 2015, 34, 3079–3089.
- 33 S. Vijjamarri, V. K. Chidara and G. Du, *ACS Omega*, 2017, 2, 582–592.
- 34 C. Li, X. Hua, Z. Mou, X. Liu and D. Cui, *Macromol. Rapid Commun.*, 2017, 38, 1700590.
- 35 L. J. Morris, M. S. Hill, M. F. Mahon, I. Manners, F. S. McMenemy and G. R. Whittell, *Chem. Eur. J.*, 2020, 26, 2954–2966.
- 36 X.-Y. Zhai, X.-Q. Wang and Y.-G. Zhou, *Eur. Polym. J.*, 2020, 134, 10982.
- 37 X.-Q. Wang, X.-Y. Zhai, B. Wu, Y.-Q. Bai and Y.-G. Zhou, *ACS Macro Lett.*, 2020, 9, 969–973.
- 38 J. M. Blackwell, K. L. Foster, V. H. Beck and W. E. Piers, *J. Org. Chem.*, 1999, 64, 4887–4892.
- 39 D. J. Parks, J. M. Blackwell and W. E. Piers, *J. Org. Chem.*, 2000, 65, 3090–3098.
- 40 M. Rubin, T. Schwiser and V. Gevorgyan, *J. Org. Chem.*, 2002, 67, 1936–1940.
- 41 Y. Ma, B. Wang, L. Zhang and Z. Hou, *J. Am. Chem. Soc.*, 2016, 138, 3663–3666.
- 42 D. J. Harrison, R. McDonald and L. Rosenberg, *Organometallics*, 2005, 24, 1398–1400.
- 43 D. W. Kim, S. Joung, J. G. Kim and S. Chang, *Angew. Chem. Int. Ed.*, 2015, 54, 14805–14809.
- 44 C. S. Sample, S.-H. Lee, M. W. Bates, J. M. Ren, J. Lawrence, V. Lensch, J. A. Gerbec, C. M. Bates, S. Li and C. J. Hawker, *Macromolecules*, 2019, 52, 1993–1999.
- 45 K. Matsumoto, Y. Oba, Y. Nakajima, S. Shimada and K. Sato, *Angew. Chem. Int. Ed.*, 2018, 57, 4637–4641.
- 46 C. Li, L. Wang, M. Wang, B. Liu, X. Liu and D. Cui, *Angew. Chem. Int. Ed.*, 2019, 58, 11434–11438.
- 47 J. M. Blackwell, D. J. Morrison and W. E. Piers, *Tetrahedron*, 2002, 58, 8247–8254.
- 48 M. Karplus, *J. Am. Chem. Soc.*, 1963, 85, 2870–2871.
- 49 J. C. Hoch and C. M. Dobson and M. Karplus, *Biochemistry*, 1985, 24, 3831–3841.
- 50 J. Chojnowski, S. Rubinsztajn, W. Fortuniak and J. Kurjata, *J. Inorg. Organomet. Polym. Mat.*, 2007, 17, 173–187.
- 51 S. Chandrasekhar, G. Chandrasekar, M. S. Reddy and P. Srihari, *Org. Biomol. Chem.*, 2006, 1650–1652.